



Seismic performance of conventional construction I-shape brace members and their bolted connections

Alina Rudman¹, Robert Tremblay², Colin Rogers³

¹ Master's student, Department of Civil Engineering and Applied Mechanics, McGill University - Montréal, QC, Canada.

² Professor, Department of Civil, Geological and Mining Engineering, Polytechnique Montréal - Montréal, QC, Canada.

³ Professor, Department of Civil Engineering and Applied Mechanics, McGill University - Montréal, QC, Canada.

ABSTRACT

The seismic design of steel structures involves the principles of capacity design, which take advantage of the inelastic ductility of the Seismic Force Resisting System (SFRS) to dissipate seismic energy. However, there exists the Conventional Construction (CC) category of SFRS in the National Building Code of Canada and the CSA S16 Standard, for which the engineer is allowed to waive capacity design principles and design a SFRS which is expected to behave principally elastically when subjected to design-level earthquakes. For Type CC steel braced frames the energy dissipation is not restricted to yielding and buckling of the braces; it can also develop through localized yielding in connections and through friction within these joints. In moderate and high seismic regions, the CSA S16 Standard requires the engineer to increase the design seismic forces for connections by a factor of 1.5, if it cannot be demonstrated that the connections in the lateral load path have an expected failure mode that is ductile. This has proven to be challenging to engineers because no guidelines or recommendations are readily available to determine the ductility of connections. While Type CC braced frames are used extensively throughout the country, there is very little research available to give insight into the ductility of these systems, particularly in the case of I-shape braces with bolted end connections. The objective of this research was to measure the inelastic response of Type CC full-scale I-shape braces and their bolted connections under reversed-cyclic seismic loading. Six brace specimens comprising two commonly used bolted connection types were designed following the provisions in CSA S16 without any capacity design rules. The paper includes a summary of the laboratory test program. The test measurements indicated that Type CC brace specimens could achieve storey drift ratios of 1%-2%, even though capacity based design provisions were not incorporated in their design.

Keywords: steel braces, conventional construction, bolted connections, laboratory testing, seismic loading.

INTRODUCTION

In Canada, the seismic design of steel structures involves the principles of capacity design, which rely on the inelastic ductility of defined components in the Seismic Force Resisting System (SFRS) to dissipate seismic energy. Specific to concentrically braced frames (CBFs), the moderately ductile (MD) and limited ductility (LD) categories both require that seismic energy be dissipated through yielding of bracing members, and that the other members and connections in the lateral load path be designed for the probable capacity of the braces in tension and compression. However, there also exists the Conventional Construction (CC) category, as listed in Table 4.1.8.9 of the National Building Code of Canada (NBCC) [1] and as outlined in Clause 27.11 of the CSA S16 Standard [2], for which the engineer is allowed to waive capacity design principles and design a SFRS which is expected to behave principally elastically when subjected to design-level earthquakes. These Type CC systems are designed using low R-values ($R_o = 1.3$ & $R_d = 1.5$), and hence do not depend on extensive yielding concentrated in specially detailed fuse elements to dissipate earthquake energy. Instead, energy dissipation is assumed to occur through limited yielding in members and connections along the lateral load path, as well as through friction within the joints. However, in moderate and high seismic zones, the CSA S16 Standard requires the engineer to increase by a factor of 1.5 the design seismic forces for the connections in the lateral load path if it cannot be demonstrated that these connections have an expected failure mode that is ductile. This has proven to be challenging to engineers because no guidelines or recommendations are given to determine the ductility of connections. As a result, quantifying the level of ductility of these components becomes an important factor in designing Type CC systems under seismic loading.

While Type CC braced frames are used extensively throughout the country, there is very little research available to give insight into the ductility of these systems, particularly in the case of I-shaped braces with bolted end connections. As such, the objective of this research was to measure the response of I-shape braces and their bolted connections under reversed-cyclic seismic loading. Six full-scale brace specimens were tested. This included two I-shape section sizes, which are frequently used for high-

rise and industrial buildings. Additionally, two commonly used bolted connection types were tested: one with plates transferring the load from the I-shape to the gusset plate and the other using angles for this purpose. These connections were designed following the provisions in CSA S16 without any capacity design rules. The 1.5 factor penalty from CSA S16 Clause 27.11 [2], i.e. the seismic design forces for the connections based on $R_d R_o = 1.3$, was not included in the design, assuming that the connections would develop sufficient ductility. Finally, the initial excursion in the loading protocol was varied between compression and tension to observe what impact this would have on overall brace / connection behaviour and ductility. The loading protocol itself was developed using statistical data from a nonlinear numerical study of five buildings designed with Type CC braced frames subjected to site representative seismic ground motions.

TESTING PROGRAM

The objective of the laboratory testing was to design, build and test six braces with two common bolted connection types (Figure 1), to observe and evaluate their behaviour and ductility, and to address the lack of previous experimental data of full-scale Type CC braces. The maximum size of the selected I-shapes was limited by the capacity of the testing equipment (Figure 2b). I-shapes of sizes W360×134 and W310×97 (ASTM A992 Gr. 50) were selected. These sections are compact and are of common depths for diagonals in multistorey and industrial buildings. Compact I-shape sections are preferred for use as braces because of the smaller difference between the tension and compression capacities. The factored compression resistance (buckling) of the braces as determined using CSA S16 Cl. 13.3 [2] was used as the strength requirement to design the brace end connections, given that the full building seismic load calculation was not available. This approach was taken because the design buckling resistance was assumed to be the limiting selection factor for a brace in a typical CBF building. The resistances of the braces were 2209 kN (W310×97) and 3680 kN (W360×134), assuming a buckling length of $KL = 6$ m using a corner-to-corner length of 6.67 m (Figure 2a) multiplied by a K factor of 0.9. The global brace slenderness values were 78 and 45 for the W310×97 section and 64 and 38 for the W360×134 section, for minor and major axis buckling, respectively. In reviewing end configurations currently used in the industry for I-shape braces, two common bolted brace end connections were selected for testing in this study. The two connections are herein named the jaw plate connection (connected by a plate at each flange of the I-shape (Figures 1a & 2c)) and the claw angle connection (connected by two angles at each flange of the I-shape (Figures 1b & 2d)). While the angles were bolted on both sides of the connection, the jaw plates were welded on the side of the gusset plate. All connections included two splice plates connecting the web of the I-shape to the gusset plate to minimise shear lag effects. Further, two web plates were used as opposed to one to eliminate additional eccentricity at the connection. Rectangular gusset plates were selected as opposed to tapered gusset plates. In addition to being easier to design and manufacture, rectangular gusset plates have shown less tearing under cyclic loading as compared to tapered gusset plates due to lower stress concentrations [3]. However, in a finite element parametric study, these have shown less ductility in a frame than tapered gusset plates [4] but allow for the attainment of greater tensile and compressive resistances. A listing of the connection design parameters for the test specimens is provided in Table 1. A complete description of the connection design procedure is provided in the work of Rudman [5].

The I-shape braces in this project were fabricated with ASTM A992 gr. 50 steel, the plates were fabricated with ASTM A572 50 steel, and the angles were fabricated with ASTM A6 gr. 44 steel. The nominal yield stress (F_y) for the braces and the plates was 345 MPa, while the nominal tensile stress (F_u) was 450 MPa. For the angles, the nominal F_y was 300 MPa and the nominal F_u was 450 MPa. Measured material properties were all above the nominal values; see Rudman [5] for a complete listing.

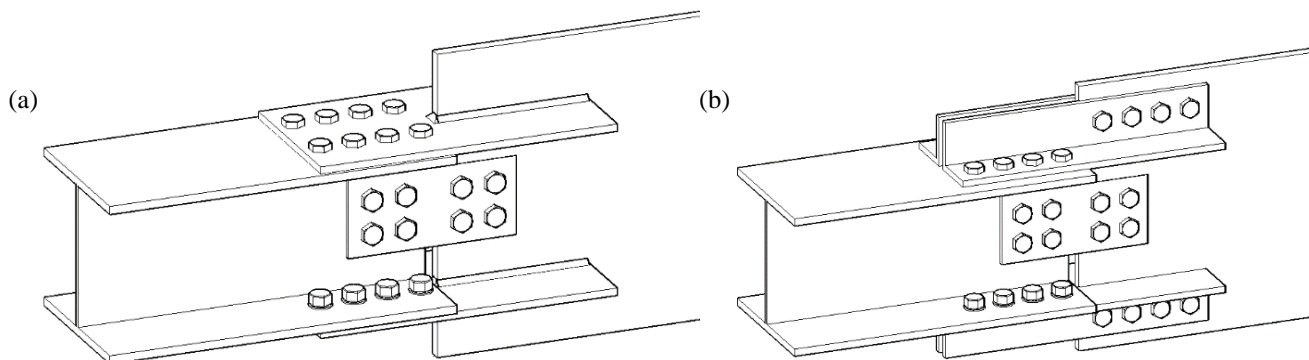


Figure 1. Standard bolted I-shape connections: (a) jaw plate connection, (b) angle connection.

The loading protocol was developed based on information obtained from a pre-testing numerical study, in which five Type CC CBF structures were designed for Vancouver and Montreal on soil class E and C. The software ETABS [6] was used for the nonlinear dynamic analysis of the model buildings, which were subjected to a suite of scaled ground motions selected for the city of interest. The nonlinear behaviour of the braces and end connections was modeled, given information available from past

test programs and numerical models of connections and braces. The deformation demands in the brace connections were obtained, and then used to create a representative reversed-cyclic loading protocol. The ATC-24 protocol [7] was found to best replicate the demands from the numerical model; however, since it was developed for site class D, and for buildings other than Type CC CBFs, the number of cycles and amplitudes of displacements were modified to match the statistical review of the results obtained from the ETABS models. Each specimen was tested in duplicate with the difference being the initial direction of the loading protocol. The first of two nominally identical specimens was tested with the loading protocol starting in tension, while the second specimen was tested with the loading protocol reversed to start in compression. The purpose was to evaluate the effect of the direction of the first loading excursion on these I-shape specimens with bolted end connections. A detailed description of the loading protocol and its development is provided by Rudman [5].

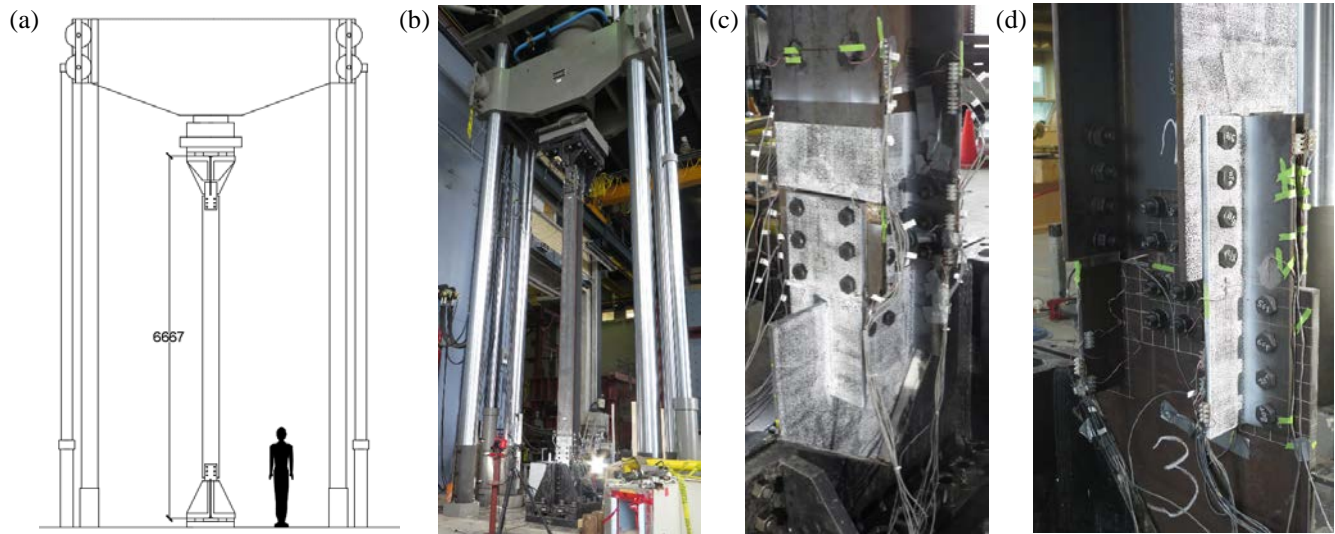


Figure 2. Brace test assembly in 12MN universal testing machine: (a) schematic drawing, (b) full setup, (c) bottom jaw plate connection, (d) bottom angle connection.

Table 1. Summary of brace and connection test specimen design parameters.

Design Element	Parameter	J310 ^a	J360 ^a	C360 ^a
Brace	Size	W310×97	W360×134	W360×134
Bolts	Grade	A325	A490	A490
	Size (in.)	7/8	1	1
	No. rows per flange	3	4	4
	No. rows in web	2	2	2
Bolt spacing	End distance (mm)	32	38	38
	Spacing (mm)	76	76	76
	Gauge in flanges (mm)	146	152	178
	Gauge in web (mm)	76	76	76
Angles	Section	NA	NA	L127×127×16
	Gauge 1 (mm)	NA	NA	76
	Gauge 2 (mm)	NA	NA	76
Web plates	Width (mm)	140	156	156
	Thickness (mm)	9.5	9.5	9.5
Jaw plates	Width (mm)	219	349	349
	Thickness (mm)	16	16	16
Welds	D (mm)	8	11	11
	Length (mm)	4 × 241	4 × 343	4 × 343
Gusset plates	Thickness (mm)	16	19	25

^a “J” indicates Jaw plate connection (Figure 1a) and “C” indicates Angle connection (Figure 1b)

The tests were performed in the Structural Engineering Laboratory at Polytechnique Montreal using the test setup developed for previous similar tests [8]. The 12 MN MTS load frame (Figure 2b) captures displacement data with an internal LVDT and load

data via a 12 MN load cell. MTS Series 793 software was used to control the press, while the MTS TestSuite Multipurpose Elite software was used to implement the loading protocol. In addition to data recorded by the MTS software, three types of instrumentation were used to capture data during the tests: string potentiometers and linear potentiometers for axial and out-of-plane displacements, strain gauges for local strains, and the digital image correlation (DIC) system for the bottom connection (Figures 2C & 2D). The measurement instruments (except the DIC system) were connected to Vishay Model 6100 scanners that were used to record data at ten scans per second using the Vishay System 6000 StrainSmart software. At the bottom of the brace, three digital image correlation camera setups (Correlated Solutions Inc.) were used to capture the movements of a speckle pattern that was painted onto the visible portion of the gusset plate, the connecting plates, and the bottom of the brace on the North, South, and East sides. Each camera setup consisted of two Sony ICX625 cameras (type CCD 2/3" 5MP FireWire): one camera positioned at an angle above the connection and the other positioned at an angle below the connection. The VIC-Snap version 8 software was used for the image capture. These images were then processed in VIC3D version 8 to extract the displacements and strains at a precision of approximately $50\mu\epsilon$ (depending on the proximity of the set-up to the specimen). See Rudman [5] for the specifics of the test setup and instrumentation.

TEST OBSERVATIONS AND RESULTS

A visual summary of the damage patterns observed for the jaw plate connection test specimens (J310 and J360) is provided in Figure 3, while similar information is shown in Figure 4 for the angle connection test specimens (C360). The axial load vs. overall displacement for each of the six test specimens is shown in Figures 5 - 7. A summary of the measured elongations in tension of each test specimen, including elongation, storey drift ratio, elastic elongation component and inelastic elongation component, at P_y , P_u , $0.8P_u$ and $0.5P_u$ is found in Table 2. Lastly, the calculated specimen ductility during tension cycles, as defined by the ratio δ_u/δ_y is given in Table 3. A detailed description of the laboratory test program can be found in the work of Rudman [5].

The J310 jaw plate connection specimens exhibited inelastic deformations in the brace member and the connections. The brace underwent local and overall minor axis buckling during compression cycles (Figure 3a), while the gusset plates also rotated during this component of loading. While undergoing the tension cycles the brace would straighten and extensive inelastic deformations were observed in the web of the I-shape (block shear Figure 3c) and the net section of the flange plate (Figure 3b). In addition, the bolts connecting the flanges to the flange plates failed in shear; noticeable shear deformations of these fasteners occurred prior to their fracture. Figure 5 illustrates that the buckling capacity was reached, followed by a significant reduction in compression resistance in the post-buckling range. However, during the tension cycles, the yield plateau was reached repeatedly, especially for the specimen that was loaded in compression during the first cyclic excursion. The difference in the tension response of the two differently loaded specimens, J310-T vs. J310-C, is thought to be due to the slow tension cycle that was applied in an attempt to identify yielding for the J310-T specimen, which was the first to be tested. Bolt slip was also evident whenever the direction of loading was reversed; this did provide for additional energy dissipation in the connections. Even though the flange bolts did fail in shear, the overall inelastic deformations were significant (see Table 3) considering that capacity protection procedures were not implemented in the design of the brace and its connections.

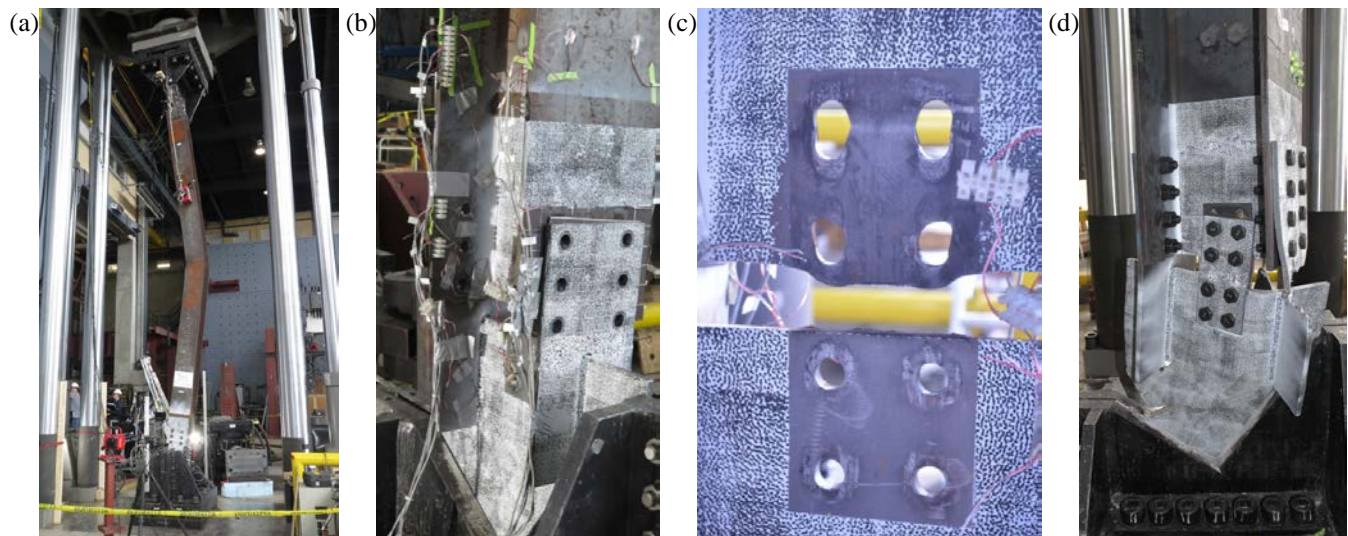


Figure 3. Typical observed damage in jaw plate connections: (a) overall & local brace buckling (J310-C), (b) shear fracture of flange bolts (J310-T), (c) block shear of web (J310-T), (d) gusset plate out-of-plane deformation and jaw plate fracture (J360-T).

The larger jaw plate connection specimens, J360, also exhibited inelastic deformations during the two loading protocols that were applied. However, overall buckling of the braces during compression cycles was not observed. Instead, damage under compression loading was largely restricted to the gusset plates, which laterally translated out-of-plane (Figure 3d), giving rise to large inelastic straining. This translation also resulted in some local buckling of the brace flanges near the end connections; likely brought about to accommodate for the movement of the gusset plates. The jaw plates yielded under tension loading, which in one case was followed by fracture of this component (Figure 3d). Block shear failure of the web in the I-shape also occurred, similar to the J310 specimens (Figure 3c). Due to the extensive plastic straining of the gusset plates during compression cycles, progressive fracture of these plates was observed during the subsequent tension cycles (Figure 3d). Figure 6 illustrates a similar response to that observed for the J310 specimens; a typical buckling peak is reached during compression loading, but this was limited by the capacity of the gusset plates and their lateral translation. Once this compression peak was reached, the post-peak capacity decreased quite rapidly. During the tension cycles, the yield plateau was reached over repeated cycles. The decay in the tension resistance as high displacements were applied was due to the progressive fracture of the gusset plates. In the case of J360-T, this fracture occurred more quickly than for J360-C, hence the additional tension cycles that can be seen in Figure 6b. Bolt slip was also evident whenever the direction of loading was reversed; it again proved to benefit the ability of the connections to dissipate energy. As with the smaller jaw plate connections, the overall inelastic deformations of the J360 specimens were substantial (see Table 3) given that the design of the test specimens did not promote the use of ductile detailing. Bolt shear fracture was not observed.

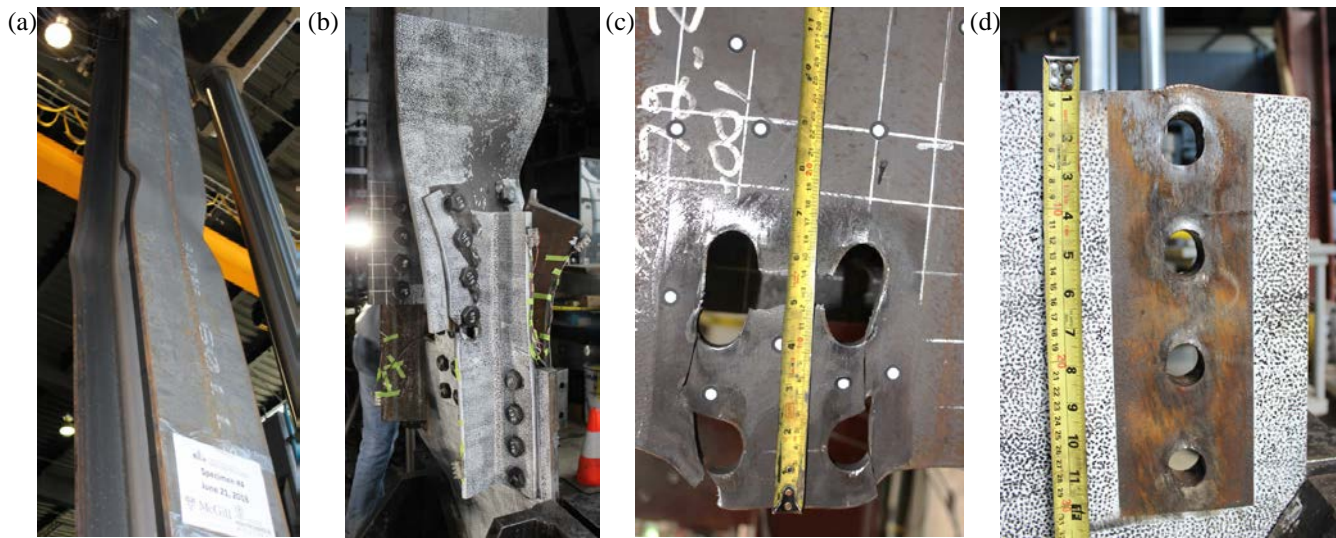


Figure 4. Typical observed damage in angle connections: (a) overall & local brace buckling (C360-C), (b) angle block shear and gusset plate out-of-plane deformation (C360-T), (c) block shear of web (C360-T), (d) gusset plate bearing (C360-C).

The test specimens connected with four angles at each end (C360) illustrated the many ways that inelastic deformations can develop, both in the connections and braces (Figure 4). Under compression cycles, separate behaviours were observed for the two specimens. As seen in Figure 4a, for test C360-C overall minor axis brace buckling with local buckling of the flanges (mid-length) was observed. This was accompanied by some rotation of the gusset plates at each end of the brace. In contrast, test C360-T did not suffer from overall brace buckling while loaded in compression. Instead, lateral translation of the gusset plates occurred (Figure 4b); some local deformation of the brace flanges near the connection was also observed, again a result of the lateral movement of the gusset plate. This result shows the sensitivity of the compression failure mode to the imperfections associated with fabrication and installation. These two specimens were nominally identical. However, the gusset plates being slightly out-of-vertical for test C360-T resulted in their lateral movement under compression, rather than buckling of the brace. It should be noted that the capacities associated with these two failure modes were very similar (Figure 7), which is why only a small eccentricity resulted in the change in behaviour. The post-peak compression resistance decreased rapidly for both specimens; this behaviour was independent of the failure mode. In terms of tension cycle response to loading, both specimens performed similarly; bearing damage to the gusset plates at bolt holes was observed (Figure 4d). More evident was the block shear failure of the legs of the connecting angles (Figure 4b) and the block shear failure of the web of the I-shape. Nonetheless, these specimens were subjected to repeated cycles in tension before a loss in resistance was seen due to the development of these block shear failure modes. Bolt shear fracture was not observed. Bolt slip was however evident whenever the direction of loading was reversed, as found for the other brace connection configurations; it also proved to benefit the ability of the connections to dissipate energy. As with the jaw plate connections, the overall inelastic deformations of the C360 specimens were substantial (see Table 3) even though a different connection detail was utilized.

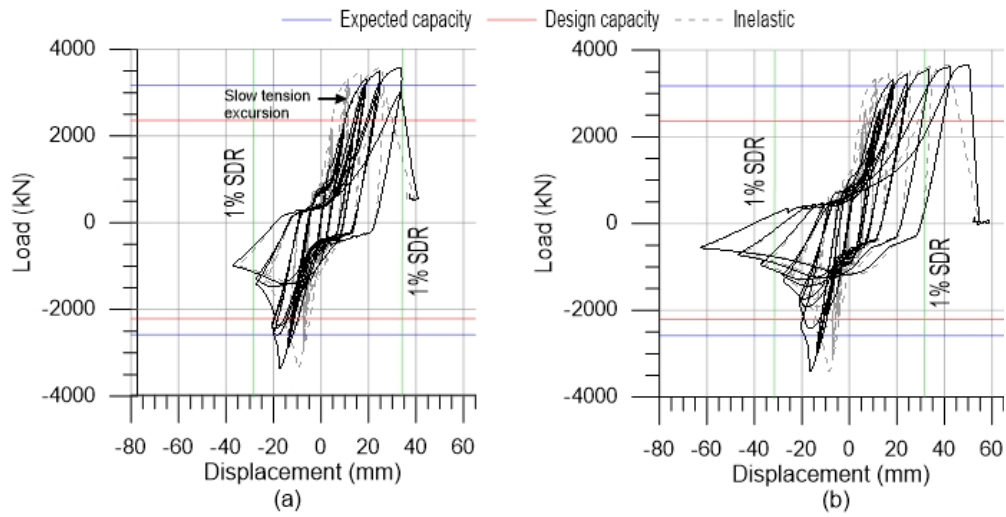


Figure 5. J310 (jaw plate conn.) axial load vs. overall displacement: (a) -T 1st cycle tension, (b) -C 1st cycle compression.

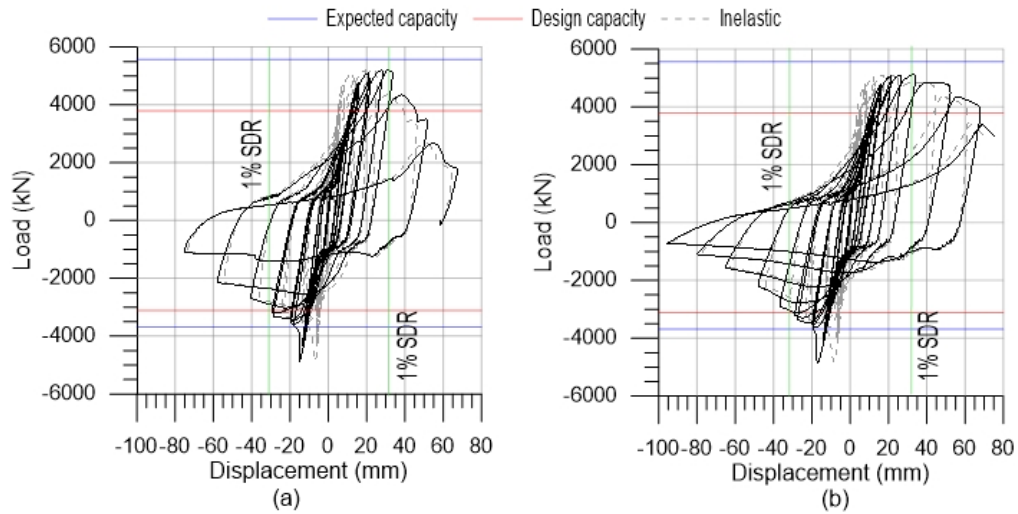


Figure 6. J360 (jaw plate conn.) axial load vs. overall displacement: (a) -T 1st cycle tension, (b) -C 1st cycle compression.

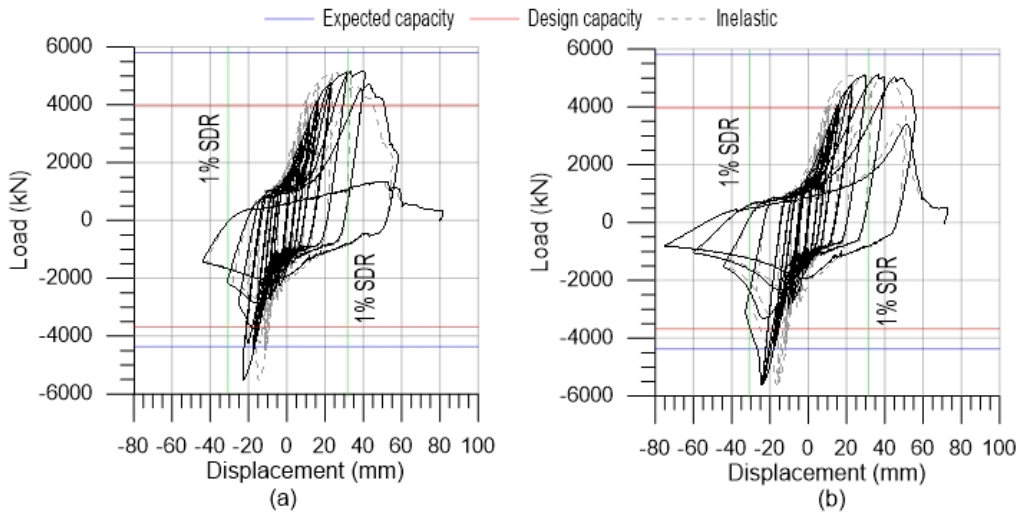


Figure 7. C360 (angle conn.) axial load vs. overall displacement: (a) -T 1st cycle tension, (b) -C 1st cycle compression.

The general shape of the axial load vs. overall displacement hysteretic curves for all six specimens resembled that of a typical capacity protected brace, in which the connections would not suffer from inelastic damage. The tension yielding component of these curves may not have been as extensive as that associated with a brace that fully yields along its length, however, the potential for these Type CC braces and connections to function in a ductile fashion is evident. Measurements of the elongation listed in Tables 2 and 3 show that these specimens were capable of reaching storey drift ratios of 1%-2%, even though capacity based design provisions were not incorporated in their design.

Table 2. Measured elongations in tension at P_y , P_u , $0.8P_u$ and $0.5P_u$.

	Load	J310-T	J310-C	J360-T	J360-C	C360-T	C360-C
Elongation (mm)	P_y	17.9	18.5	19.7	19.7	20.0	19.4
	P_u	33.3	49.9	31.2	33.0	40.6	36.6
	$0.8P_u$	34.1	51.4	42.0	65.6	50.5	55.0
	$0.5P_u^a$	36.9	52.6	52.5	75.2	55.3	54.4
Storey drift ratio (%)	P_y	0.58	0.60	0.63	0.64	0.64	0.63
	P_u	1.07	1.61	1.01	1.06	1.31	1.18
	$0.8P_u$	1.10	1.66	1.36	2.12	1.63	1.77
	$0.5P_u^a$	1.19	1.70	1.69	2.43	1.78	1.76
Elastic component ^b (mm)	P_y	7.5	7.7	8.3	8.7	6.4	6.2
	P_u	8.2	8.5	8.7	9.0	7.4	7.3
	$0.8P_u$	6.6	7.0	15.0	7.3	5.9	5.8
	$0.5P_u^a$	4.1	4.2	4.3	5.3	0.6	3.7
Inelastic component ^c (mm)	P_y	10.4	10.8	11.4	11.0	13.6	13.2
	P_u	25.1	41.4	22.5	24.0	33.2	29.3
	$0.8P_u$	27.5	44.4	27.0	58.3	44.6	49.2
	$0.5P_u^a$	32.8	48.4	48.2	69.9	54.7	50.7

^a $0.5P_u$ or the last recorded elongation value if $0.5P_u$ was not attained during the test

^bElastic component is simplified as the elastic elongation of the I-shape only

^cInelastic component is the difference between the full elongation and the elastic elongation of the I-shape

Table 3. Calculated specimen ductility (tension loading cycles).

	J310-T	J310-C	J360-T	J360-C	C360-T	C360-C
δ_u/δ_y	1.86	2.70	1.59	1.67	2.03	1.88

CONCLUSIONS

Reversed-cyclic testing of six full-scale Type CC brace specimens was carried out to evaluate their ability to develop inelastic deformations for seismic resistance. Two common bolted connection types were included in the scope of study; the jaw plate connection and the angle connection. The specimens exhibited an ability to carry load in the nonlinear range due to an assortment of inelastic deformations in both the braces and connections. Damage was due to overall and local brace buckling, tension yielding of jaw plates, angles and gusset plates, block shear failure of brace webs and angles, bolt fracture and fracture of the gusset plates. The friction forces associated with bolt slip also provided for energy dissipation capability. The load direction of the first excursion did not make a significant impact on the overall behaviour of the tested specimens. However, specimens which were first loaded in compression were able to achieve more cycles before fracture or significant loss of load carrying capacity than their nominally identical specimen. The test measurements indicated that the Type CC brace specimens were able to achieve storey drift ratios of 1%-2%, even though capacity design provisions were not incorporated in their design. However, prior to drawing general conclusions as to the performance of all Type CC brace connections additional research on braces with bolted end connections will need to be carried out. Further numerical analysis, in particular, will allow for a better understanding of the results found in this study. This should include a parametric study using advanced finite element models to cover the range of brace sizes and connection types. Following the characterization of the typical CC brace connections, their influence on the overall response of a building to seismic loading should be evaluated to verify the use of the current R-values for design and the requirement to design brace connections using $R_d R_o = 1.3$.

ACKNOWLEDGMENTS

The authors would like to thank the ADF Group Inc. and DPHV Structural Consultants for their generous technical and financial support, as well as the Natural Sciences and Engineering Research Council of Canada, the Fonds de recherche du Québec - Nature et technologies and the Centre d'études interuniversitaire des structures sous charges extrêmes. The authors also express their appreciation to the technical staff of the Structural Engineering Laboratory at Polytechnique Montreal.

REFERENCES

- [1] National Research Council of Canada (NRCC) (2015). *National Building Code of Canada (NBCC)*, 13th ed., Ottawa, ON, Canada.
- [2] Canadian Standards Association – CSA (2014). *CSA S16-14: Design of steel structures*. Toronto, ON.
- [3] Roeder, C.W., Lehman, D.E., and Clark, K. (2011) “Influence of gusset plate connections and braces on the seismic performance of X-braced frames”. *Earthquake Engineering & Structural Dynamics* 40(4): 355-74.
- [4] Alipour, M., and Aghakouchak, A.A. (2013) “Numerical analysis of the nonlinear performance of concentrically braced frames under cyclic loading”. *International Journal of Steel Structures* 13(3): 401-19.
- [5] Rudman, A. (2018). “Testing of conventional construction W-shape brace members and their bolted end connections undergoing reversed cyclic loading.” Master’s thesis, Department of Civil Engineering, McGill University, Montreal.
- [6] Computers and Structures Inc. (CSI) (2018) *ETABS Ultimate v. 17.0.1*. Walnut Creek, CA, USA.
- [7] Applied Technology Council (ATC) ATC-24 (1992) “Guidelines for cyclic seismic testing of components of steel structures for buildings”. Report No. ATC-24, Redwood City, CA, USA.
- [8] Tremblay, R., Haddad, M., Martinez, G., Richard, J., and Moffatt, K. (2008). “Inelastic cyclic testing of large size steel bracing members.” Proceedings of the 14th World Conference on Earthquake Engineering, Beijing, China, Paper No. 05-05-0071.